SEISMIC BEHAVIOR OF SHORT GFRP-RC CIRCULAR COLUMNS

Amr E. Abdallah[1], Ehab F. El-Salakawy[2]

[1] PhD Candidate, Department of Civil Engineering, University of Manitoba, Winnipeg, Manitoba, Canada; Assistant Lecturer, Department of Civil Engineering, Assiut University, Assiut, Egypt.
E-mail: abdalla3@myumanitoba.ca
[2] Professor, Department of Civil Engineering, University of Manitoba, Winnipeg, Manitoba, Canada.
E-mail: Ehab.El-Salakawy@umanitoba.ca

ABSTRACT

The available provisions for seismic design of fiber-reinforced polymer-reinforced concrete (FRP-RC) columns were fundamentally derived from design models created for steel-RC ones due to the limited research data on the former. This, in turn, may justify the conservativeness of such provisions, particularly those concerning the design of confinement reinforcement for FRP-RC columns with different shear span-to-depth ratios. This study investigates the effect of shear span-to-depth ratio and axial load level on the seismic response of columns reinforced with glass FRP (GFRP) by testing four full-scale GFRP-RC circular columns under earthquake-simulated loading. A versatile test setup was utilized to enable quasi-static lateral loading along with constant axial loading regardless of the column shear span. The tested short columns failed in flexure although the theoretical analysis predicted a shear type of failure. The experimental results revealed that unlike steel-RC columns, changing the shear span-to-depth ratio insignificantly influenced the hysteretic response of GFRP-RC columns, indicating that the available code provisions for confinement reinforcement and shear design are overly strict.

Keywords: Glass fiber-reinforced polymer (GFRP), hysteretic response, circular columns, shear span-to-depth ratio, axial load level.

INTRODUCTION

The widespread acceptance of the non-corroding fiber-reinforced polymer (FRP) reinforcement for use in reinforced concrete (RC) structures, as a substitute for conventional steel reinforcement, requires independent design provisions implementing the properties of FRP reinforcement. In other words, the design provisions of steel-RC members cannot be extended to FRP-RC ones because of the behavioral differences. These include, but are not limited to, the absence of yielding plateau, relatively low modulus of elasticity and behaving linearly elastic up to failure for FRP. These properties made the effectiveness of FRP-RC structures in earthquake-prone zones questionable. However, this was refuted later by recent research studies [1-6]. Despite their inclusion of design provisions for various structural members such as slabs, flat plates and beams [7-9], column design provisions are still developing at a much slower pace because of the limited availability of experimental data. For example, the ACI 440.1R-15 [7] guidelines do not permit using FRP as main reinforcement in compression members, whereas the Canadian standards CSA S806-12 [8] neglect the contribution of FRP reinforcement in columns. The Canadian code, CSA S6-19 [9] recognizes the contribution of FRP in compression with an upper limit of 0.002 compressive strain.
Many research studies were conducted to investigate the performance of FRP-RC columns under static loading [10-13], where glass FRP (GFRP) was utilized due to its relatively low cost and sufficient strain capacity. Yet, the available research data on the seismic response of FRP-RC columns is rather limited [1-6, 14]. Stable hysteretic behavior was reported for well-confined GFRP-RC columns with satisfactory energy dissipation levels. In addition, the deformability of GFRP-RC columns compensated for the ductility of steel-RC columns. Using GFRP in lieu of steel decreased the shear and moment capacities

of columns, whereas the deformability and member behavior were enhanced [14]. The current design provisions for transverse reinforcement spacing were reported to be too conservative [2, 6], which could be a result of deriving the current design equation of the Canadian standards CSA S806-12 [8] directly from a design model developed for steel-RC columns [15]. This model assumed that the shear span-to-depth ratio is proportional to the drift capacity of the column under seismic loading, following the conclusions of previous work on steel-RC columns [16-18]. Later, this assumption was rebutted for steel-RC columns [19]. Yet, the effect of shear span-to-depth ratio has not been evaluated yet for GFRP-RC columns, except for few attempts that used fiber-reinforced concrete, other FRP types or hybrid reinforcement configurations [20-22]. This study aimed to investigate the effect of shear span-to-depth ratio and axial load level on the seismic performance of GFRP-RC columns. Additionally, a modified version for the current equation for confinement reinforcement design in the Canadian standards CSA S806-12 [8] was proposed.

EXPERIMENTAL PROGRAM

Materials

Ready-mixed, normal-weight concrete having a target compressive strength of 35 MPa at 28 days was used to cast all specimens. To identify the actual concrete compressive strength, standard 100 × 200-mm concrete cylinders were prepared and tested as per CSA A23.1-19/A23.2-19 [23] on testing day of each column, as listed in Table 1. All specimens were reinforced longitudinally and transversally using sand-coated GFRP size No. 16 bars (15.9-mm diameter) and size No. 10 spirals (9.5-mm diameter), respectively. The physical and mechanical properties of the used GFRP bars and spirals are summarized in Table 2, as reported in the product datasheets issued by the manufacturer [24] or as obtained from laboratory testing, as applicable [8].

Table 1: Properties of test specimens

Specimen ID	Shear span-to-depth ratio, L/D	Axial load level, P/P_o	Cracking load applied kN	Concrete strength, f_c' MPa	Average length of hinging region, L_i mm
G-3.0-0.2	3.0	0.2	47	44.2 $\pm$ 0.1	407
G-3.0-0.3	3.0	0.3	85	45.9 $\pm$ 0.7	460
G-5.0-0.2	5.0	0.2	24	36.9 $\pm$ 0.4	525
G-5.0-0.3	5.0	0.3	30	41.4 $\pm$ 0.7	525

Table 2: Mechanical properties of GFRP reinforcement

Bar type	Nominal diameter mm	Area mm^2	Modulus of elasticity GPa	Tensile strength MPa	Ultimate strain (%)
No. 16	15.9	197.9[a] (235)[b]	65.7[c]	1,711[d]	2.60[d]
No. 10 (Spirals)	9.5	71[a] (83)[b]	58.4[c]	1,376[d, e]	2.36[d, e]

[a] Nominal area according to CSA S807-19 [25].
[b] Actual area measured as per Annex A of CSA S806-12 [8].
[c] Calculated in accordance with Annex C of CSA S806-12 [8].
[d] Calculated using nominal area and average force as per Annex C of CSA S806-12 [8].
[e] Obtained from tests on straight bars from the same batch following Annex C of CSA S806-12 [8].

Test Specimens

The test program incorporated casting and testing of Four full-scale column-footing connections were constructed and tested under concurrent axial loading and cyclic lateral drift reversals. Each column had a rigid 1,400 × 900 × 600-mm footing, properly reinforced with 15M (16-mm diameter) steel bars, to provide rotational fixity for the column during testing. Each test specimen represented the lower portion of a column between the column-footing interface and the theoretical point of contra-flexure, such as a first-story column in a multi-story moment-resisting frame (MRF) or a bridge column bent in double curvature. All columns had a circular cross-section with a diameter of 350 mm. The shear span, defined herein as the distance between top surface of the footing and the line of action of applied lateral load, was either 1,050 or 1,750 mm, resulting in a shear span-to-depth ratio of 3.0 or 5.0, respectively. The larger shear span-to-depth ratio represented typical column height whereas the lower shear span-to-depth ratio resembled short bridge piers or captive columns in (MRFs) [26]. The design of test specimens was carried out as per CSA S806-12 [8], CSA S6-19 [9], and the recommendations of recent research studies [2, 6, 21], as appropriate. All columns had a spiral pitch of 85 mm as per Clause 12.7.3.4 of CSA S806-12 [8]. Investigating the seismic response of short GFRP-RC columns with an shear span-to-depth ratio of 3.0 was of interest since they were theoretically found to fail in shear when analyzed using the actual lateral load capacity of other columns tested earlier [6] in accordance with the shear design provisions of CSA S806-12 [8]. Following the common construction practice, the test specimens were constructed in two consecutive pours, starting with the footings. For each shear span-to-depth ratio, a column was subjected to an axial load level of 0.2 and another one was tested under an axial load level of 03. Two specimens tested by the authors [6] were used for comparison against the short columns tested in this study.
The specimens were labelled using a three-character alphanumeric code. The first letter, G, denoted the GFRP reinforcement used for all columns. The second number referred to the column shear span-to-depth ratio, while the last fraction represented the applied axial load level. The latter was expressed as the ratio of the applied axial load, P, to the nominal unconfined axial capacity of the GFRP-RC column, P_o. The details of the tested specimens are listed in Table 1.

Test setup and procedure

Three main elements comprised the test setup (Fig. 1); the hydraulic actuator, the axial loading frame and the RC supporting blocks. The horizontal hydraulic actuator, having $\pm$ 1,000-kN and $\pm$ 250-mm load and displacement capacities, respectively, was anchored to an RC reaction wall and used to apply the cyclic lateral loads or drifts. The positive sign indicated that the applied load or drift was pushing the column whereas negative sign was used when the load or drift was pulling the column. The axial loading was applied through a 2,000-kN load capacity hydraulic jack. The reactions of the axial load were transferred to the laboratory strong floor through a hinged steel loading frame (two hollow steel section (HSS) links pinned to a steel spreader I-beam) pinned to two RC blocks at the bottom. An RC slab was used below each specimen to align the actuator with the anticipated line of action of lateral loading or drifting. Post-tensioned high-strength threaded bars were utilized to anchor the footing, RC slab and blocks to the laboratory strong floor. For each shear span-to-depth ratio, a different set of HSSs and RC supporting blocks were used.
The test started by applying the specified axial load, where the axial load was calculated as a ratio of the nominal unconfined axial capacity of the column, P_o; calculated as per the Canadian standards [8]:

$$P_o = \alpha_1 \phi_c f_c^{'} (A_g - A_F) \quad \text{Eq.1}$$

where α_1 is the average stress in the rectangular compression block compared to the specified concrete strength, f_c'; ϕ_c is the resistance factor for concrete, which was taken as unity; A_g is the gross cross-sectional area of the column; and A_F is the total area of the main FRP reinforcement.
Following the application of the axial load, two load-controlled cycles were applied to identify the lateral cracking load and represent the column at service stage. Afterwards, the lateral drift history was applied to the columns, following the recommendations of ACI 374.1-05 [27]. Quasi-static reversible lateral drift cycles were applied at a frequency of 0.01 Hz with three identical cycles, in terms of the drift ratio for each drift step. The drift ratio is defined herein as the lateral displacement of at mid-height of the column

head as a percentage of the column shear span. A load-controlled service cycle was applied after each drift step beyond 2.00% drift ratio to assess the stiffness degradation, if any [2, 4, 6]. The tests were terminated when the specimens exhibited a lateral load resistance less than 75% of the maximum lateral load capacity experienced.

Fig. 1: Test setup

EXPERIMENTAL RESULTS AND DISCUSSION

General Behavior and Mode of Failure

The lateral load at first cracking increased as the axial load level increased or as the shear span-to-depth ratio decreased, which is clearly shown in Table 1. Concrete cover spalling took place during a drift ratio of 2.00% for G-3.0-0.3 and G-5.0-0.3 and 3.00% for G-3.0-0.2, G-5.0-0.2. The failure drift was not affected by the variation of the shear span-to-depth ratio, which agreed with the finings of Deng. et al. [21] for GFRP-RC columns cast using fiber-reinforced concrete. However, this contradicted with the observations of Sharbatdar [20] for CFRP-RC columns, where shorter columns exhibited less drift capacities. The average length of hinging region for the specimens, as listed in Table 1, were directly proportional to shear span-to-depth ratio with an insignificant effect for the axial load level. This contradicted the reported relationship between Such a nearly-linear relationship between column aspect ratio and length of hinging region for length of hinging region and shear span-to-depth ratio for steel-RC columns [17]. The hinge length-to-column diameter ratios had an upper bound for shear span-to-depth ratio at approximately 4.0 for steel-RC columns, beyond which slight change of hinge length-to-column diameter ratio could be noticed.

All columns failed in flexure, as shown in Fig. 2. Higher intensity of shear cracks was noticed for the short columns, which concurred with the reported results of Sharbatdar [20] for CFRP-RC columns. However, the rate of strength degradation for G-3.0-0.2 and G-3.0-0.3 was similar to that of their longer counterparts. This suggests that the available code provisions for shear design in CSA S806-12 [8] are too conservative for GFRP-RC columns under seismic-loading conditions. Failure was characterized for specimens G-3.0-0.2, G-5.0-0.2, and G-5.0-0.3 by simultaneous concrete core crushing and compression failure of an outermost longitudinal bar, followed by failure of another two bars on the compression side for G-3.0-0.2. Specimen G-3.0-0.3 exhibited a combination of concrete core crushing, three-bar delamination and spiral rupture at failure.

Table 3: Theoretical and experimental lateral load and drift capacities

Specimen ID	Theoretical capacity		Experimental lateral capacity		
	Lateral load kN	Drift [a] (%)	Maximum kN	At failure kN	Strength Degradation (%)
G-3.0-0.2	90.0	5.20	+158.0 at 4.00% drift -181.5 at -8.15% drift	-111.9 at -10.00% drift	38.3
G-3.0-0.3	96.7	3.11	+189.1 at 4.00% drift -195.5 at -5.00% drift	+98.7 at 6.17% drift	47.8
G-5.0-0.2	54.0	5.20	+94.1 at 4.00% drift -96.0 at -10.20% drift	+58.8 at 10.20% drift	37.5
G-5.0-0.3	58.0	3.11	+101.2 at 2.00% drift −77.5 at -2.00% drift	+73.0 at 6.50% drift	27.9

[a] Calculated according to Clause 12.7.3.3 of CSA S806-12 (CSA 2017).

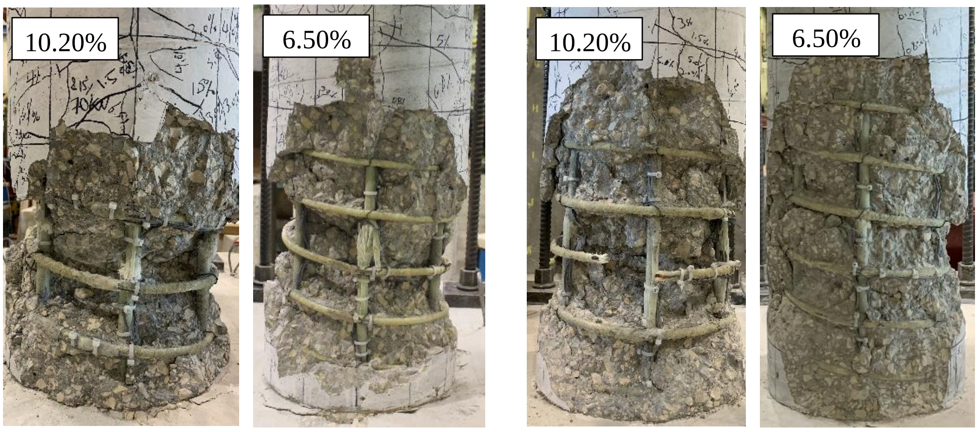

(a) G-3.0-0.2 (b) G-5.0-0.2 (c) G-3.0-0.3 (d) G-5.0-0.3

Fig. 2: Test specimens at failure

Hysteretic Response

The initial stiffnesses were similar for all specimens as they had similar concrete strengths. The lateral load resistance was significantly decreased as the shear span-to-depth ratio increased (Fig. 3). The lateral load capacity increased by 14, and 8% when the axial load level increased from 0.2 to 0.3 P_o for shear span-to-depth ratio of 3.0, and 5.0, respectively, accompanied by rapid strength decay and less deformable behavior.
The effect of increasing axial load level was comparable for both shear span-to-depth ratios tested in this study, resulting in a 36% decrease in failure drift. All specimens exceeded the drift ratio limit for ductile MRFs, which is equal to 4.00% [8]. Due to the variation of column shear span, the hysteretic responses of the specimens were compared in terms of bending moment at the interface, instead of lateral load, versus drift ratio. The moment at the critical section was calculated following the approach of Tavassoli et al. [1].
Increasing the shear span-to-depth ratio had marginal influence on the moment and drift capacities. This indicates the conservative nature of the available code provisions for seismic design of confinement reinforcement in FRP-RC columns, since those provisions assumed inferior deformability for shorter columns. Table 3 lists the experimental and theoretical load capacities and failure drifts.

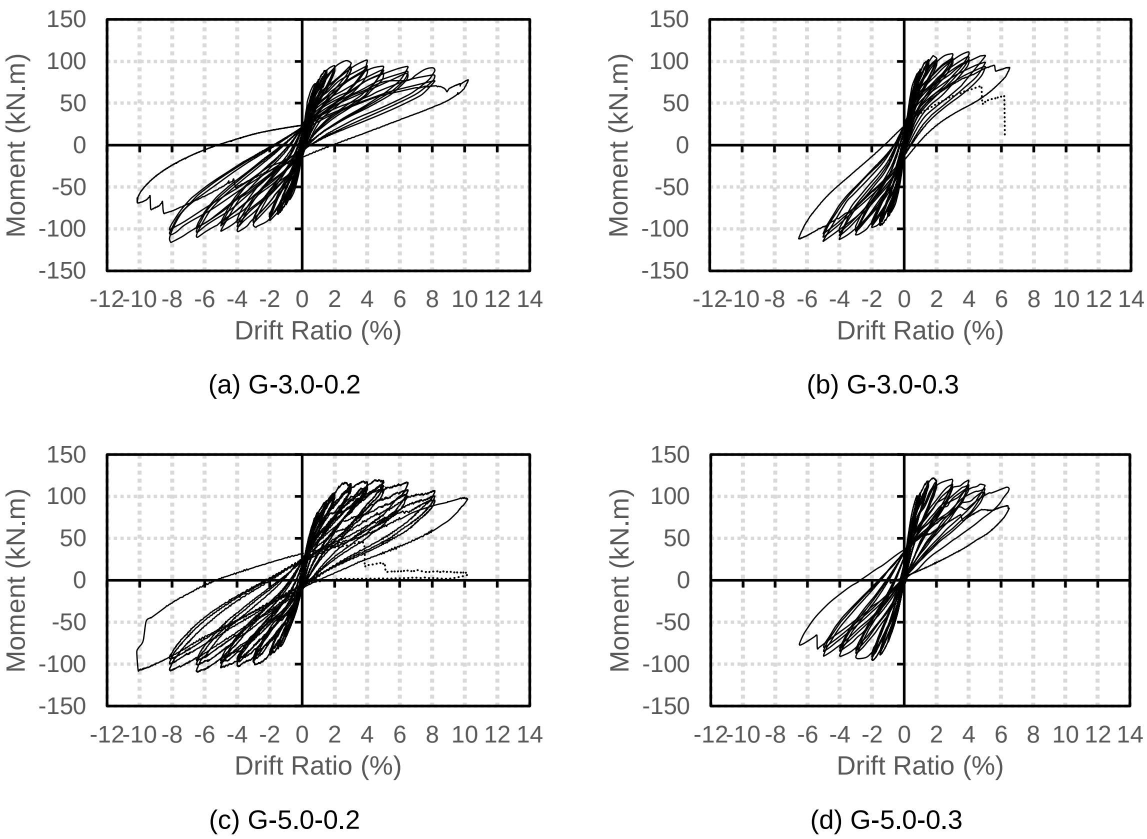

(a) G-3.0-0.2 (b) G-3.0-0.3

(c) G-5.0-0.2 (d) G-5.0-0.3

Fig. 3: Hysteresis diagrams for test specimens

CONCLUSIONS

Based on the experimental results of this study, the following conclusions can be drawn:

1. The design equation in Clause 12.7.3.3 of CSA S806-12 [8] for confinement reinforcement of FRP-RC columns in seismic-active zones is too strict. This can be attributed to the assumption that columns with smaller shear span-to-depth ratios are less deformable. Such assumption is inapplicable to GFRP-RC columns. Thus, the aforementioned design equation should be adjusted according to the current knowledge.
2. Increasing the shear span-to-depth ratio significantly decreased in the lateral load capacity, whereas the drift capacity was not influenced. A similar effect to the latter was noticed for the moment capacity. Unlike steel-RC columns, the shear span-to-depth ratio was directly proportional to hinge length-to-column diameter ratio for GFRP-RC columns.
3. Both columns with the shear span-to-depth ratio of 3.0 exhibited flexure-controlled failure despite the shear failure anticipated from the theoretical shear analysis according to the Canadian standards for FRP-RC structures [8]. This indicates that the current shear design provisions in the Canadian standards are overly conservative.
4. Increasing the axial load level from 0.2 to 0.3 of the nominal unconfined axial capacity of the columns increased lateral load capacity accompanied with rapid strength degradation and lower deformability. The failure drift was decreased by 36% for the tested columns as a result of increasing the axial load level. Furthermore, increasing the axial load level enhanced the moment capacity at the critical section by 11 and 7% for shear span-to-depth ratio equal to 3.0, and 5.0, respectively. However, the variation of axial load level hardly affected the hinge length-to-column diameter ratio.

ACKNOWLEDGEMENTS

The authors would like to express their gratitude to the Natural Sciences and Engineering Research Council of Canada (NSERC) and the University of Manitoba Graduate Fellowship (UMGF) for their generous financial support. The assistance received from the technical staff at the W. R. McQuade Heavy Structures Laboratory at the University of Manitoba is appreciated.

REFERENCES

1. Tavassoli, A., Liu, J., and Sheikh., S. (2015). "Glass fiber-reinforced polymer-reinforced circular columns under simulated seismic loads." *ACI Struct. J.* Vol. 112 (1): pp. 103–114.
2. Ali, M. A., and El-Salakawy, E. (2016). "Seismic performance of GFRP-reinforced concrete rectangular columns." *J. Compos. Constr.* Vol. 20 (3): pp. 04015074.
3. Elshamandy, M. G., Farghaly, A. S., and Benmokrane, B. (2018). "Experimental behavior of glass fiber-reinforced polymer-reinforced concrete columns under lateral cyclic load." *ACI Struct. J.* Vol. 115 (2): pp. 337–349.
4. Hasaballa, M., and El-Salakawy, E. (2018). "Anchorage performance of GFRP headed and bent bars in beam-column joints subjected to seismic loading." *J. Compos. Constr.* Vol. 22 (6): pp. 04018060.
5. El-Gendy, M. G., and El-Salakawy, E. F. (2020). "GFRP shear reinforcement for slab-column edge connections subjected to reversed cyclic lateral load." *J. Compos. Constr.* Vol. 24 (2): pp. 04020003.
6. Abdallah, A. E. M., and El-Salakawy, E. (2021). "Confinement properties of GFRP-reinforced concrete circular columns under simulated seismic loading." *J. Compos. Constr.* ASCE, Vol. 25 (2): pp. 04020088.
7. ACI. (2015). "Guide for the design and construction of structural concrete reinforced with fiber-reinforced polymer (FRP) bars." ACI 440.1R-15, *American Concrete Institute,* Farmington Hills, MI.
8. CSA. (2017). "Design and construction of building structures with fibre-reinforced polymer." CSA S806-12 (R2017). *Canadian Standards Association (CSA)*, Toronto, ON.
9. CSA. (2019). "Canadian highway bridge design code." CSA S6-19." *Canadian Standards Association (CSA)*, Toronto, ON.
10. Tobbi, H., Farghaly, A. S., and Benmokrane, B. (2014). "Behavior of concentrically loaded fiber-reinforced polymer reinforced concrete columns with varying reinforcement types and ratios." *ACI Struct. J.* Vol. 111 (2): pp. 375–386.
11. Guérin, M., H. M. Mohamed, B. Benmokrane, A. Nanni, and Shield, C. K. (2018). "Eccentric behavior of full-scale reinforced concrete columns with glass fiber-reinforced polymer bars and ties." *ACI Struct. J*. Vol. 115 (2): pp. 489-499.
12. Liu, J., H. Du, H. Zhou, Z. Nan, and Nie, P. (2019). "Experimental study on deformation and failure of circular concrete columns reinforced with glass fiber–reinforced polymer bars." *ACI Struct. J.* Vol. 116 (4): pp. 45–52.
13. Barua, S. and El-Salakawy, E. (2020). "Performance of GFRP-reinforced concrete circular short columns under concentric, eccentric, and flexural loads." *J. Compos. Constr*. Vol. 24 (5): pp. 04020044.
14. Kharal, Z., and Sheikh, S. A. (2020). "Seismic behavior of square and circular concrete columns with GFRP reinforcement." *J. Compos. Constr.* Vol. 24 (1): pp. 04019059.
15. Saatcioglu, M., and Razvi, S. R. (2002). "Displacement-based design of reinforced concrete columns for confinement." *ACI Structural Journal*. Vol. 99 (1): pp. 3-11.
16. Sakai, K., and Sheikh, S. A. (1989). "What do we know about confinement in reinforced concrete columns? (A critical review of previous work and code provisions)." *ACI Structural journal*, Vol. 86 (2): pp. 192-207.
17. Razvi, S. R., and M. Saatcioglu. 1996. "Design of R/C columns for confinement based on lateral drift." Ottawa Carleton Earthquake Engineering Research Center, Carleton, Ottawa.
18. Lehman, D. E., and Moehle, J. P. (2000). "Seismic performance of well-confined concrete bridge columns." *Pacific Earthquake Engineering Research Center*, pp. 295.
19. Bae, S., and Bayrak, O. (2008). "Seismic performance of full-scale reinforced concrete columns." *ACI Struct. J.* Vol. 105 (2): pp. 123–133.
20. Sharbatdar, M. K. (2003). "Concrete columns and beams reinforced with FRP bars and grids under monotonic and reversed cyclic loading." *Doctoral Dissertation*, University of Ottawa, Ottawa, Canada.

21. Deng, Z., Gao, L., and Wang, X. (2018). "Glass fiber-reinforced polymer-reinforced rectangular concrete columns under simulated seismic loads." *Journal of the Brazilian Society of Mechanical Sciences and Engineering*, Vol. 40 (2): pp. 111.1-111.12.
22. Kharal, Z., Carrette, J. K., and Sheikh, S. A. (2021). "Large concrete columns internally reinforced with GFRP spirals subjected to seismic loads." *J. Compos. Constr.* Vol. 25 (3), pp. 04021014.
23. CSA. (2019). "Concrete materials and methods of concrete construction/test methods and standard practices for concrete." CSA A23.1-19/A23.2-19. *Canadian Standards Association (CSA)*, Toronto, ON.
24. Pultrall Inc. (2019). "V-ROD—Technical data sheet." *ADS Comp. Group*. Thetford Mines, QC, Canada.
25. CSA. (2019). "Specification for fibre-reinforced polymers." CSA S807-19. *Canadian Standards Association (CSA)*, Toronto, ON.
26. Saatcioglu, M. 1991. "Deformability of reinforced concrete columns." *Earthquake-Resistant Structures—Inelastic Response and Design, SP-127, American Concrete Institute*, Vol. 127: pp. 421–452.
27. ACI. (2019). "Acceptance criteria for moment frames based on structural testing and commentary." ACI 374.1-05(19). *American Concrete Institute*, Farmington Hills, MI.